# High-$J_c$ $YBa_2Cu_3O_{7-\delta}$ superconducting film grown by laser-assisted chemical vapor deposition using a single liquid source and its microstructure

Pei Zhao[1], Akihiko Ito[1,*], Takeharu Kato[2],
Daisaku Yokoe[2], Tsukasa Hirayama[2], Takashi Goto[1]

[1]*Institute for Materials Research, Tohoku University, Katahira 2-1-1, Aoba-ku, Sendai 980-8577, Japan*
[2]*Japan Fine Ceramic Center, Mutsuno 2-4-1, Atsuta-ku, Nagoya 456-858, Japan*

**corresponding author: e-mail: itonium@imr.tohoku.ac.jp*
*tel: +81-22-215-2106; fax: +81-22-215-2107*

**Abstract:** A $YBa_2Cu_3O_{7-\delta}$ (YBCO) film was prepared on a multilayer-coated Hastelloy C276 substrate by laser-assisted metalorganic chemical vapor deposition using a single liquid source precursor. A *c*-axis-oriented YBCO film was grown epitaxially on a (100) $CeO_2$ layer at the deposition rate of 11 μm $h^{-1}$. A screw dislocation and stacking faults were observed in the cross section of the YBCO film. The critical current density of the YBCO film reached 2.7 MA $cm^{-2}$.

Short title: High-$J_c$ YBCO film grown by laser CVD using a single liquid source
74.62.Bf Effects of material synthesis, crystal structure, and chemical composition
68.55.-a Thin film structure and morphology
81.15.Gh Chemical vapor deposition (including plasma-enhanced CVD, MOCVD, etc.)
74.78.Bz High-Tc films



**Please cite this manuscript as:**

P. Zhao, A. Ito, T. Kato, D. Yokoe, T. Hirayama, T. Goto: High-$J_c$ $YBa_2Cu_3O_{7-\delta}$ superconducting film grown by laser-assisted chemical vapor deposition using a single liquid source and its microstructure, Superconductor Science and Technology 26 095016 (2013). doi:10.1088/0953-2048/26/9/095016

## 1. Introduction

Conductors coated with the high-temperature superconductor $YBa_2Cu_3O_{7-\delta}$ (YBCO) have been fabricated by various techniques, such as metal organic deposition using trifluoroacetates [1], pulsed laser deposition [2], and metalorganic chemical vapor deposition (MOCVD) [3,4]. Among these techniques, MOCVD is promising for the preparation of coated conductors because it not only provides a high deposition rate and uniform coverage but can also be adapted to a reel-to-reel deposition system for the fabrication of long-length wires.

A laser-assisted MOCVD (laser CVD) is advantageous for the preparation of oriented films at high deposition rates [5–7]. We prepared *c*-axis-oriented YBCO film on a multilayer-coated Hastelloy C276 tape at a high deposition rate of 55 μm $h^{-1}$ [8]. This YBCO film exhibited a critical current density ($J_c$) of 0.5 MA $cm^{-2}$. For industrial applications, a high critical current density ($J_c$) greater than 1 MA $cm^{-2}$ and high adaptability to a continuous production are required. In the previous study, Y, Ba, and Cu solid compounds were used as precursors, and the composition of the precursor vapor was independently controlled by varying the evaporation temperature of each precursor. However, a constant feed of multi-component vapor through the evaporation of solid precursors is difficult because of agglomeration and sintering, *i.e*., changes in the surfaces of the precursors and the corresponding degradation of their surface state. However, the use of a liquid precursor to continuously and stably supply a precursor at a constant rate for a prolonged period is feasible.

Miyata *et al*. recently reported the high-rate preparation of YBCO superconducting films using laser CVD [9]. They also studied the mechanism of growth mode in laser CVD process taking into account of the relationship between deposition rate and precursor delivery rate, while the microstructure of high-$J_C$ film prepared by laser CVD has not been elucidated.

In this study, we report the high-speed preparation of a high-$J_c$ YBCO film exhibiting 2.7 MA $cm^{-2}$ by laser CVD using a single liquid source precursor and its microstructure.

## 2. Experimental

$Y(DPM)_3$, $Ba(DPM)_2$/$Ba(TMOD)_2$, and $Cu(DPM)_2$ (DPM; dipivaloylmethanate and TMOD; 2,2,6,6-tetramethyl-3,5-octanedionate) precursors were dissolved in tetrahydrofuran ($C_4H_8O$; THF) at a Y concentration of 0.275 mol $L^{-1}$. The source solution was delivered into the evaporation chamber using a plunger pump at a supply rate of $0.83 \times 10^{-5}$ L $s^{-1}$. The evaporation chamber was heated to 653 K. The beam of a continuous-wave Nd:YAG laser (wavelength: 1064 μm) was defocused up to 25 mm in diameter to irradiate the whole substrate was introduced into chamber through a quartz window [6]. A multilayer-coated Hastelloy C276 tape (10 × 5 × 0.1 mm) with a structure of $CeO_2$/MgO/$Y_2O_3$/$Al_2O_3$/Hastelloy C276 was used as a substrate. The substrate was preheated at 823 K. The flow rates of Ar and $O_2$ gases were $1.52 \times 10^{-6}$ and $0.34 \times 10^{-6}$ Pa $m^3$ $s^{-1}$, respectively. The total pressure was maintained at 0.8 kPa. The deposition time was 180 s. The as-deposited YBCO films were heat treated in the sequence 573 K for 14.4 ks, 673 K

for 14.4 ks, and 773 K for 14.4 ks in a pure $O_2$ atmosphere (100 kPa) to transform the YBCO from its tetragonal to orthorhombic structure.

The phase was studied by X-ray diffraction (XRD; Rigaku RAD-2C). The out-of-plane crystallinity of the YBCO film was evaluated on the basis of the full-width at half-maximum (FWHM) of the ω-scan on the (005) reflection. The in-plane orientation was evaluated by the FWHM of the φ-scan on the (103) reflection, which was measured by a pole-figure X-ray diffractometer (XRD; Rigaku Ultima IV). The microstructure was observed using a field-emission scanning electron microscope (FESEM; JEOL JSM-7500F) and a transmission electron microscope (TEM; Topcon EM-002B). The composition was analyzed by an energy-dispersive X-ray spectrometer attached to the TEM (TEM-EDS). The schematic of the epitaxial relationship was illustrated using VESTA [10]. Ag electrodes of approximately 6-μm thickness were deposited onto the sample surface via dc sputtering and were connected to thin copper wires (dia. 0.1 mm). The critical current ($I_c$) was measured in liquid $N_2$ (77 K) using a dc four-probe method with the criterion of 1 μV $cm^{-1}$.

**3. Results and discussion**

Figure 1 shows the XRD pattern of the YBCO film prepared at a deposition temperature of 1020 K (laser power of 123 W). The YBCO film showed a *c*-axis orientation. The weak diffractions from the (100) and (200) planes suggested that a small amount of *a*-axis-oriented YBCO grains were present. A small amount of (110)-oriented $BaCuO_2$ (JCPDF #38-1402) was also observed. The FWHM of the ω-scan on the (005) reflection and that of the φ-scan on the (103) reflection of this YBCO film were 1.8° and 3.2°, respectively. These values imply that the orientation of this film was improved from that of YBCO films prepared using solid precursors in a previous study (2.0° and 3.8°, respectively) [8].

Figure 2 shows the X-ray pole figure pattern from the (103) reflection of the YBCO films and that from the (220) reflection of the $CeO_2$ layer. The pole figure of the (103) reflection of the YBCO film showed a fourfold pattern at approximately α = 44°, which was attributed to the YBCO {103} planes at a interior angle of 46° to the YBCO (001) plane. The pole figure of the (220) reflection of the $CeO_2$ film showed a fourfold pattern at approximately α = 45°, which corresponded to the $CeO_2$ {220} planes with an interior angle of 45° to the $CeO_2$ (100) plane. The azimuth angles β of the (103) reflections of the YBCO film were rotated 45° with respect to those of $CeO_2$ (220) reflections, which indicates the in-plane epitaxial growth relationship of YBCO [110] // $CeO_2$ [001].

Figure 3 shows the surface SEM images of the YBCO film and the schematic of the in-plane epitaxial relationship between the *c*-axis-oriented YBCO grains and the $CeO_2$ layer. The surface of the *c*-axis-oriented YBCO film was flat because of a coherent lattice matching between YBCO (001) and $CeO_2$ (100) planes (Fig. 3(b)). Needle-like grains (A in Fig. 3(a)) were distributed on the surface. *a*-axis-oriented YBCO grains were often found on the films as needle-like grains. Their longer directions, namely *c*-axis direction, were aligned orthogonally (Fig. 3(c)), which can be determined on the basis of X-ray pole figure and TEM

observation (Fig. 4). According to the calculation of the surface Gibbs energies of YBCO planes [11], *a*-axis orientation is much favored than *c*-axis orientation at lower deposition temperature and higher supersaturation. In addition, the increase in the amount of *a*-axis-oriented grains as the increase in the thickness of *c*-axis-oriented YBCO film has often been reported [12,13]. The *a*-axis-oriented YBCO grains were nucleated at grain boundary and surface roughness and grew larger in the *c*-axis-oriented YBCO films [14], resulted in the film surface consisting of needle-like grains and the decrease in the critical current density [12]. Outgrowth of flower-like grains were also observed (B and C in Fig. 3(a)), which were identified as Ba– and Cu–O compounds on the basis of the TEM-EDS analysis. TEM specimens of areas D were fabricated by a focused ion beam technique.

Figure 4 shows TEM images and selected-area electron diffraction (SAED) patterns of the *c*-axis oriented YBCO film. The cross-section of the YBCO film showed a dense structure with a thickness of 540 nm (Fig. 4(a), 4(b)), which indicates a deposition rate of 11 μm $h^{-1}$. The SAED pattern from the $CeO_2$ layer suggested that the <100> direction of the $CeO_2$ film was normal to the substrate surface and that the <001> direction was parallel to the cross-section (Fig. 4(d)). The SAED pattern from the film cross section indicated that the <001> direction of the YBCO film was normal to the substrate surface and that the <110> direction was parallel to the cross-section (Fig. 4(e)). The in-plane epitaxial relationship between *c*-axis-oriented YBCO film and $CeO_2$ layer was confirmed to be YBCO [110] // $CeO_2$ [001], which was the same result as the X-ray pole figure (Fig. 2). The needle-like grain, namely *a*-axis oriented YBCO grains were grown on the film surface (grain A in Fig. 4(b)). From the SAED pattern of *a*-axis-oriented YBCO grain (Fig. 4(f)), the in-plane epitaxial relationship among *a*-axis-oriented YBCO grain, *c*-axis oriented YBCO film and $CeO_2$ layer was confirmed to be *a*-YBCO [011] // *c*-YBCO [110] // $CeO_2$ [001], which was the same results as the X-ray pole figure and SEM observation (Figs. 2 and 3). The flower-like outgrowth grain was grown on the surface of *c*-axis oriented YBCO film (grain C in Fig. 4(a)), while the other grain was partially embedded in the film (grain B in Fig. 4(b)). Screw dislocations and stacking faults were identified in the dark-field cross-sectional image of the YBCO film (Fig. 4(c)). The dark-field images were taken under the **g** = 006 of YBCO condition. In this condition, dislocations having the Burgers components of the 100 or 110 directions are disappeared. Therefore, screw dislocations can be visualized because these Burgers components have the 001 direction of YBCO.

Figure 5 shows the *I*–*V* curve for the *c*-axis-oriented YBCO film. As the current was increased, the voltage initially remained zero and started to increase when the current reached to 60 A, which indicates a high $J_c$ of 2.7 MA $cm^{-2}$. The $J_c$ value obtained in the present study was greater than those of YBCO films (0.5–2.6 MA $cm^{-2}$) prepared on multilayer-coated Hastelloy C276 tape by MOCVD [16,17] and laser-assisted CVD [8,9]

A current flow in type II superconductors such as YBCO causes a transition into a mixed state. A magnetic vortex in the superconductor moves by Lorentz force, resulting in the decline in the critical current. However, non-superconducting phases distributed in the type II superconductor act as a flux pinning to

sustain high current capability [15]. Several pinning centers have been proposed: zero-dimensional point defects, one-dimensional linear defects such as screw and edge dislocations, two-dimensional planar defects such as grain boundaries and twin planes, three-dimensional defects such as secondary phase precipitations. Among them, one-dimensional pinning centers exhibit a strong pinning force against a flux line parallel to the pinning center. Because the superconducting current passes on *ab* plane of *c*-axis-oriented YBCO films, the screw dislocations perpendicular to the film might play a role of pinning center and be responsible for the enhancement of $J_c$ in the YBCO film.

## 4. Conclusions

By using laser CVD with a single liquid source precursor, we prepared a *c*-axis-oriented YBCO film that exhibited a high $J_c$ of 2.7 MA cm$^{-2}$ on multilayer-coated Hastelloy C276. The in-plane epitaxial relationship was YBCO [110] // $CeO_2$ [001]. A screw dislocation and stacking fault defects were observed in the dark-field cross-sectional image of the *c*-axis-oriented YBCO film.

## Acknowledgements

This work was supported in part by the International Superconductivity Technology Center (ISTEC). This work was also supported in part by JSPS, Grant-in-Aid for Young Scientists (A), No. 25709069, and by the 111 Project, China (B13035).

## References

[1] Izumi T, Matsuda J S, Nakaoka K, Kitoh Y, Sutoh Y, Nalkanishi T, Yoshizumi M, Yamada Y and Shiohara Y 2007 Recent Progress on R&D of Advanced TFA-MOD Process for Coated Conductors *IEEE T. Appl. Supercond.* **17** 3329–31

[2] Yamada Y, Miyata S, Yoshizumi M, Fukushima H, Ibi A, Kionoshita A, Izumi T, Shiohara Y, Kato T and Hirayama T 2009 Development of Long Length IBAD-MgO and PLD Coated Conductors *IEEE. T. Appl. Supercond.* **19** 3236 –3239

[3] Molodyk A, Novozhilov M, Street S, Castellani L and Ignatiev A 2011 All-MOCVD Technology for Coated Conductor Fabrication *IEEE T. Appl. Supercond.* **21** 3175–8

[4] Selvamanickam V, Chen Y, Kesgin I, Guevara A, Shi T, Yao Y, Qiao Y, Zhang Y, Zhang Y, Majkic G, Carota G, Rar A, Xie Y, Dackow J, Maiorov B, Civale L, Braccini V, Jaroszynski J, Xu A, Larbalestier D and Bhattacharya R 2011 Progress in Performance Improvement and New Research Areas for Cost Reduction of 2G HTS Wires *IEEE T. Appl. Supercond.* **21** 3049 –3054

[5] Ito A, Kadokura H, Kimura T and Goto T 2010 Texture and orientation characteristics of α-$Al_2O_3$ films prepared by laser chemical vapor deposition using Nd:YAG laser *J. Alloys Compd.* **489** 469–74

[6] Zhao P, Ito A, Tu R and Goto T 2010 Preparation of highly (100)-oriented $CeO_2$ films on

polycrystalline $Al_2O_3$ substrates by laser chemical vapor deposition *Surf. Coat. Technol.* **204** 3619–22

[7] Guo D, Ito A, Tu R and Goto T 2012 High-speed epitaxial growth of $BaTi_2O_5$ thick films and their in-plane orientations *Appl. Surf. Sci.* **259** 178–85

[8] Zhao P, Ito A, Kato T, Yokoe D, Hirayama T and Goto T 2013 High-speed growth of $YBa_2Cu_3O_{7-\delta}$ superconducting films on multilayer-coated Hastelloy C276 tape by laser-assisted MOCVD *Supercond. Sci. Technol.* **26** 055020

[9] Miyata S, Matsuse K, Ibi A, Izumi T, Shiohara Y and Goto T 2013 High-rate deposition of $YBa_2Cu_3O_{7-\delta}$ high-temperature superconducting films by IR-laser-assisted chemical vapor deposition *Supercond. Sci. Technol.* **26** 045020

[10] Momma K and Izumi F 2011 VESTA 3 for three-dimensional visualization of crystal, volumetric and morphology data *J. Appl. Crystallogr.* **44** 1272–6

[11] Miletto Granozio F and di Uccio U S 1997 Simple model for the nucleation of (0 0 1) and (1 0 0) oriented grains in YBCO films *J. Crystal Growth* **174** 409–16

[12] Foltyn S R, Jia Q X, Arendt P N, Kinder L, Fan Y and Smith J F 1999 Relationship between film thickness and the critical current of $YBa_2Cu_3O_{7-\delta}$-coated conductors *Appl. Phys. Lett.* **75** 3692–4

[13] Sievers S, Mattheis F, Krebs H U and Freyhardt H C 1995 Grain orientation in thick laser-deposited $Y_1Ba_2Cu_3O_{7-\delta}$ films: Adjustment of *c*-axis orientation *J. Appl. Phys.* **78** 5545–8

[14] Kato T, Sasaki H, Sasaki Y, Hirayama T, Ikuhara Y, Watanabe T, Ibi A, Iwai H, Muroga T, Miyata S, Yamada Y, Iijima Y, Kakimoto K, Sutoh Y, Saitoh T, Izumi T and Shiohara Y 2006 Nanostructural characterization of YBCO films on metal tape with textured buffer layer fabricated by pulsed-laser deposition *J. Mater. Sci.* **41** 2587–95

[15] Foltyn S R, Civale L, MacManus-Driscoll J L, Jia Q X, Maiorov B, Wang H and Maley M 2007 Materials science challenges for high-temperature superconducting wire *Nat. Mater.* **6** 631–42

[16] Watanabe T, Kashima N, Suda N, Mori M, Nagaya S, Miyata S, Ibi A, Yamada Y, Izumi T and Shiohara Y 2007 Rapid Formation of 200 m-long YBCO Coated Conductor by Multi-Stage CVD *IEEE. T. Appl. Supercond.* **17** 3386–9

[17] Stadel O, Muydinov R Y, Brauer G, Rikel M O, Ehrenberg J, Bock J, Kotzyba G, Nast R, Goldacker W, Samoylenkov S V and Kaul A R 2009 MOCVD and MOD of YBCO and Buffer Layers on Textured Metal Tapes *IEEE T. Appl. Supercond.* **19** 3160–3

**Figure captions**

**Fig. 1** XRD pattern of the YBCO film prepared on multilayer-coated Hastelloy C273 substrate at deposition temperature of 1020 K.

**Fig. 2** X-ray pole figure of the YBCO and $CeO_2$ layers for the YBCO film prepared on multilayer-coated Hastelloy C273 substrate at deposition temperature of 1020 K.

**Fig. 3** Surface SEM images of the *c*-axis-oriented YBCO film (a). Images (b) and (c) illustrate in-plane epitaxial relationship between the *c*- and *a*-axis-oriented YBCO grains and (100) $CeO_2$ plane, respectively.

**Fig. 4** TEM bright-field images (a, b), dark-field image (c) and SAED patterns (d–f) of the *c*-axis-oriented YBCO film prepared on multilayer-coated Hastelloy C273 substrate at deposition temperature of 1020 K.

**Fig. 5** *I–V* curve of the *c*-axis-oriented YBCO film prepared on multilayer-coated Hastelloy C273 substrate at deposition temperature of 1020 K.

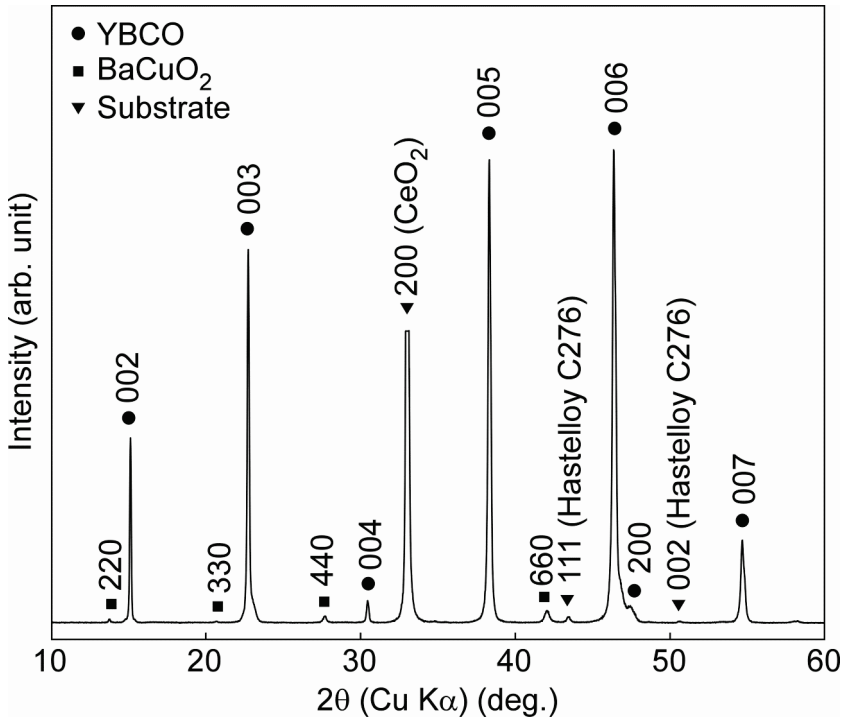


**Fig. 1** XRD pattern of the YBCO film prepared on multilayer-coated Hastelloy C273 substrate at deposition temperature of 1020 K.

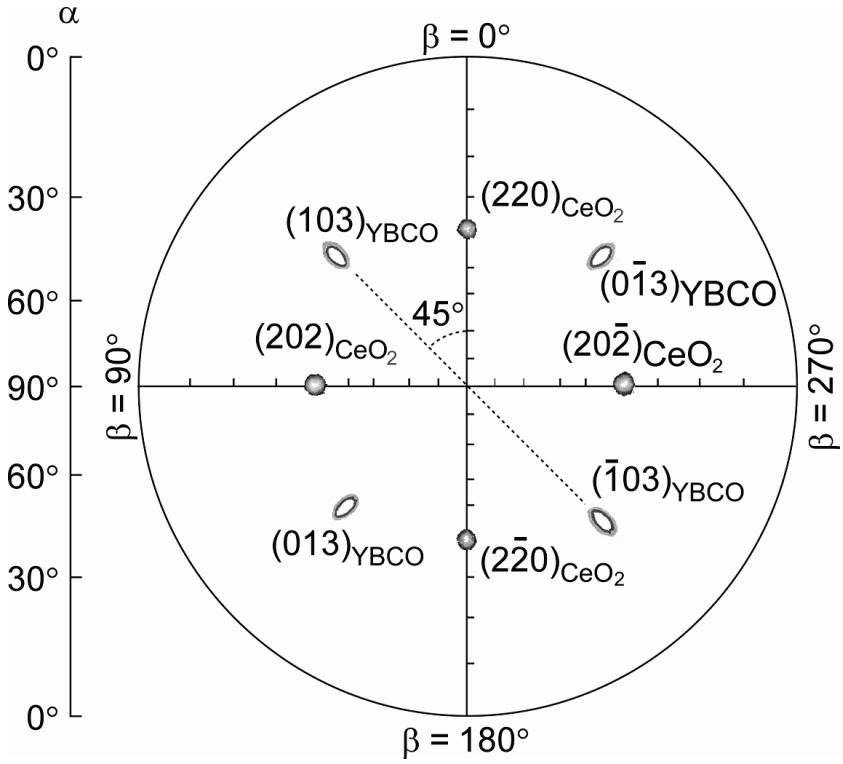


**Fig. 2** X-ray pole figure of the YBCO and $CeO_2$ layers for the YBCO film prepared on multilayer-coated Hastelloy C273 substrate at deposition temperature of 1020 K.

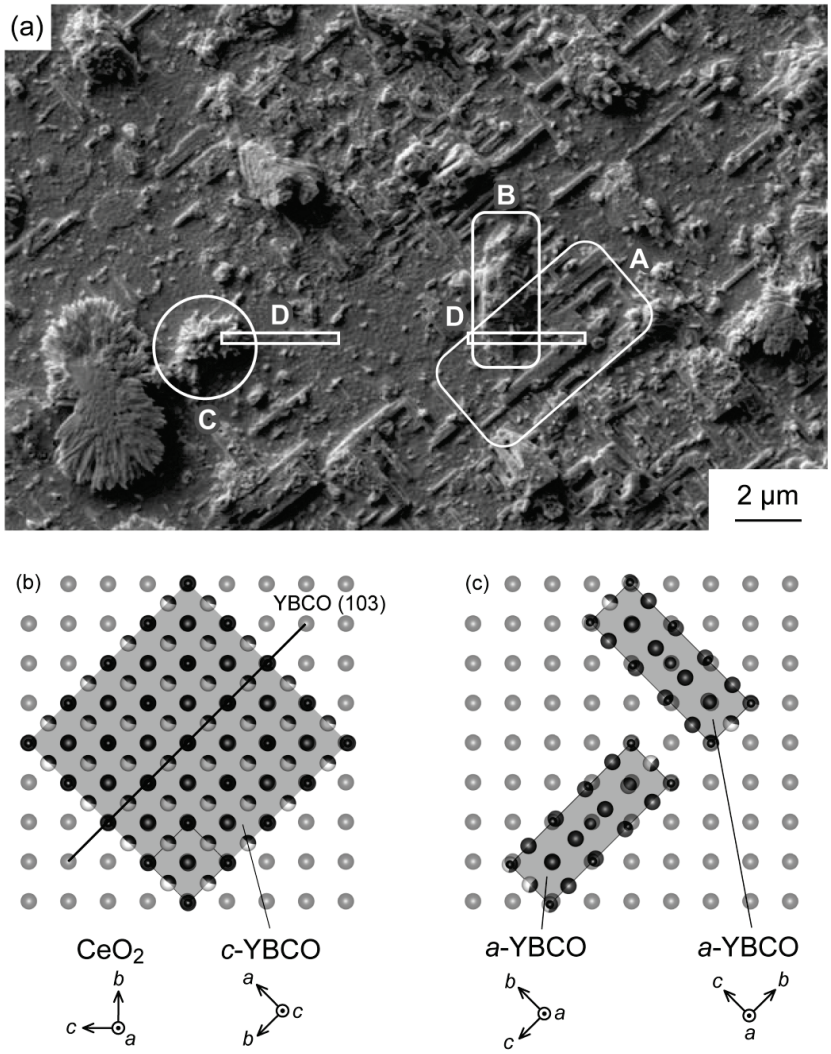


**Fig. 3** Surface SEM images of the *c*-axis-oriented YBCO film (a). Images (b) and (c) illustrate in-plane epitaxial relationship between the *c*- and *a*-axis-oriented YBCO grains and (100) $CeO_2$ plane, respectively.

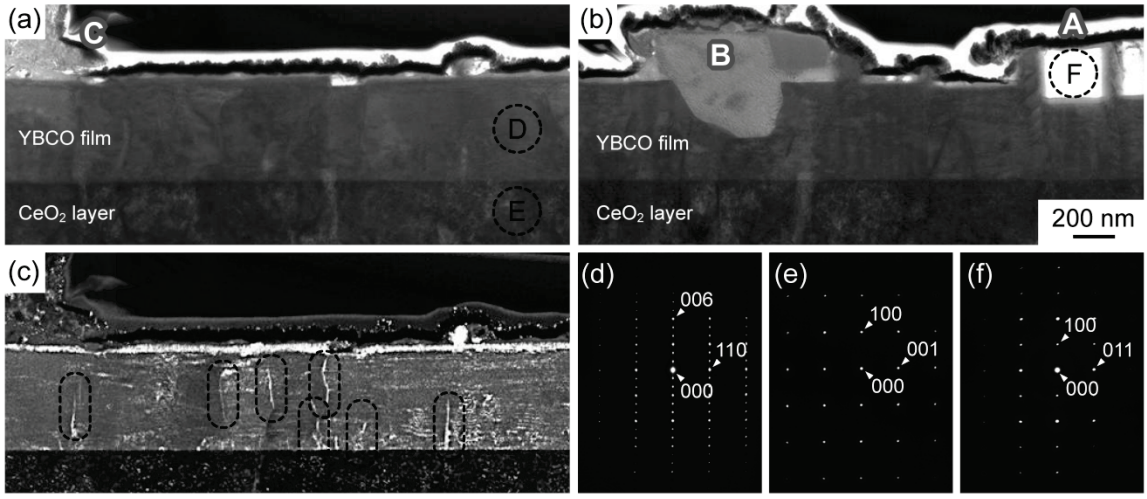


**Fig. 4** TEM bright-field images (a, b), dark-field image (c) of the *c*-axis-oriented YBCO film prepared on multilayer-coated Hastelloy C273 substrate at deposition temperature of 1020 K. SAED patterns (d-f) were taken from circles D-F, respectively.

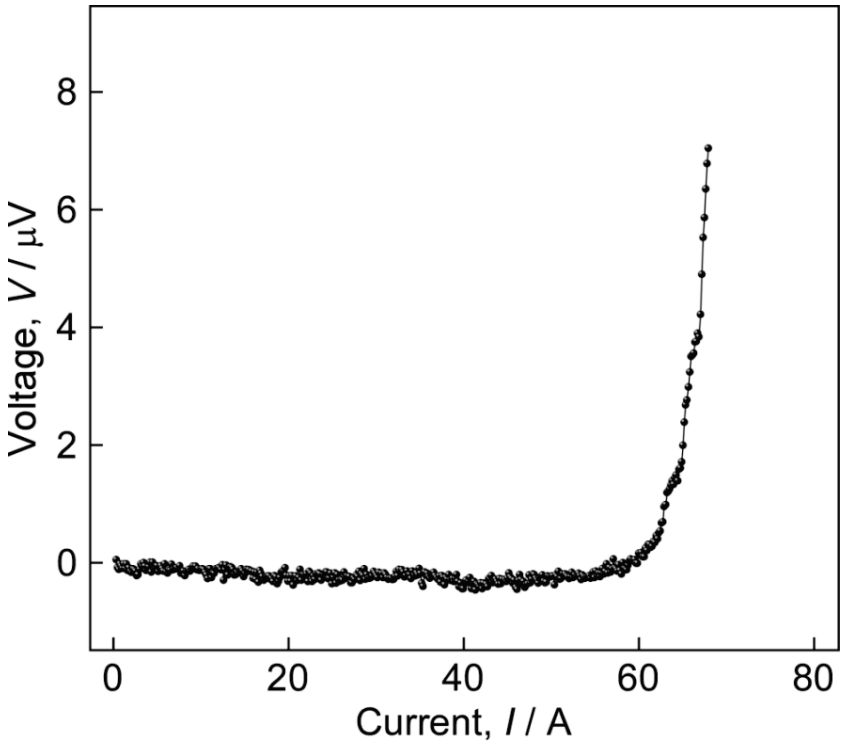


**Fig. 5** *I–V* curve of the *c*-axis-oriented YBCO film prepared on multilayer-coated Hastelloy C273 substrate at deposition temperature of 1020 K.